

THE ADVANCED MULTI-FREQUENCY RADAR (AMFR) FOR REMOTE SENSING OF CLOUDS AND PRECIPITATION

Ninoslav Majurec¹, S. M. Sekelsky¹, S. J. Frasier¹, and S. A. Rutledge²

¹University of Massachusetts, Amherst, Massachusetts

²Dept. of Atmospheric Science, Colorado State University, Ft. Collins, CO

1. INTRODUCTION

The University of Massachusetts has developed an advanced Multi-Frequency Radar (AMFR) system for studying clouds and precipitation. This mobile radar consists of three polarimetric Doppler subsystems operating at Ku-band (13.4 GHz), Ka-band (35.6 GHz) and W-band (94.92 GHz). This combination of frequency bands allows measurement of a wide range of atmospheric targets ranging from weakly reflecting clouds to strong precipitation. Beamwidths are matched at each frequency ensuring consistent sampling volume, and all systems are mounted on a programmable scanning pedestal.

AMFR employs high-power klystron amplifiers at each frequency as well as pulse compression (linear FM) in order to improve sensitivity. Range sidelobe suppression level of 45 dB is achieved using a windowing function in the receiver, while sidelobe suppression up to 60 dB is possible using amplitude tapering in both transmitter and receiver. Range resolution is 30 m (5 MHz BW). The hybrid polarization scheme is employed. Circuits for tuning the transmitted polarization and a fully complex (amplitude and phase) calibration loop have been employed together for the first time.

Although multi-frequency radar remote sensing techniques are reported in the literature, they are not widely used because few multi-frequency radars are available to the science community. One exception is the 33 GHz/95 GHz UMass Cloud Profiling Radar System (CPRS, Sekelsky 1996, 1999, 2004), which AMFR replaces. AMFR's multi-parameter capabilities are well suited for characterizing the complex microphysics of layer clouds and precipitation processes in winter storms. AMFR will also play an important role in developing algorithms and validating measurements for an upcoming generation of space-borne radars. The frequency bands selected for AMFR match those of several sensors that have been deployed or are under development. These include the Tropical Rainfall Measuring Mission (TRMM) satellite Ku-band (13 GHz) radar, the CloudSat W-band (95 GHz) radar, and the Global Precipitation Mission (GPM) satellite radars at Ku-band and Ka-band (35 GHz).

* Corresponding author address: Ninoslav Majurec, University of Massachusetts, ECE Department, 102 Knowles Eng. Bldg., 01003, Amherst, MA, Phone: 413-545-4579
E-mail: nmajurec@mirsl.ecs.umass.edu

2. SYSTEM DESCRIPTION

AMFR consists of Ku-band (13.4 GHz), Ka-band (35.6 GHz) and W-band (94.92 GHz) fully polarimetric radar subsystems, data acquisition subsystem and a truck-based mobile laboratory. Radar block schematic is shown in Figure 1. Microwave and digital electronic circuits are mounted under the antennas in weatherproof housings. Power and control signals are passed through the pedestal using a slip ring assembly and data is transmitted through a fiber optic rotary joint. This allows the AMFR to continuously rotate in azimuth. Table 1 summarizes the AMFR's specifications.

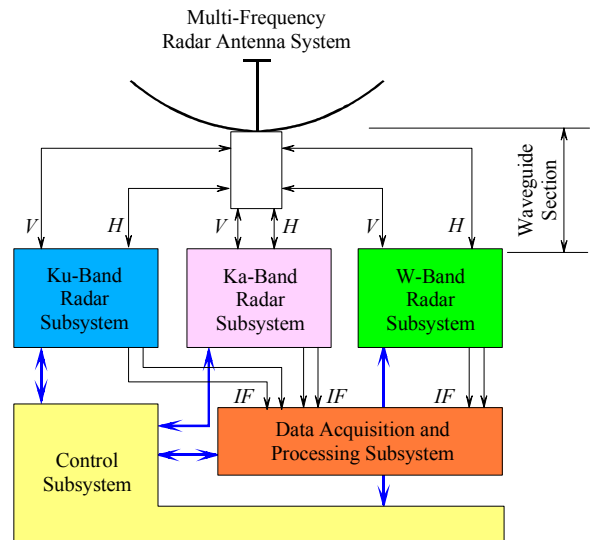


Figure 1. AMFR block schematic.

Parameter	Ku-band	Ka-band	W-band
Frequency (GHz)	13.4	35.6	94.92
Transmitted Polarization	Hybrid	Hybrid	Hybrid
Received Polarization	Hybrid	Hybrid	Hybrid
Peak Power (kW)	5	1.5	2
Pulse Compression Gain (dB)	19 max	19 max	19 max
Average Power (W)	250 [*]	50 [*]	35 [*]
Antenna	1.8 m	0.91 m	0.35 m
Antenna Gain (dB)	48	48	48
Antenna Half Power	0.75 deg	0.7 deg	0.7 deg
Beamwidth			
Range Resolution (m)	30-120	30-120	30-120
Minimum Detectable dBZe (R=1km, 1sec avg, 150m)	-54	-57	-52.5
Minimum Detectable dBZe (R=10km, 1sec avg, 150m)	-47	-50	-47.0

* Limited by latching circulators average power

Table 1. The AMFR'S Specifications

2.1 Antenna System

The AMFR antenna system consists of three separate antennas. The antennas are spaced as close as possible to avoid significant parallax. Figure 2 shows the placement of the antennas on top of the mounting plate. The Ku-band subsystem employs an Andrew HSX6-130 dual polarized (H and V) antenna. Diameter of the parabolic reflector is 6 feet (1.8 m) to ensure required beamwidth/gain design requirements listed in Table 1. The specified cross polarization is 40dB and beamwidth 0.75 degrees.

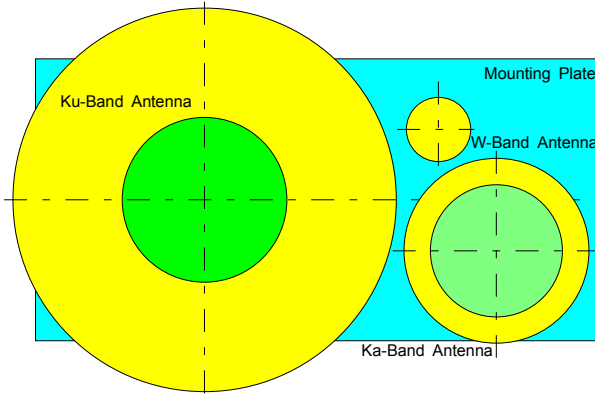


Figure 2. AMFR Antenna system (top view).

The Ka-band subsystem employs Millitech CRA-28-2 circular waveguide fed Cassegrain antenna with orthomode transducer for dual-polarization application. The diameter of the main reflector is 3 feet (0.91 m), giving expected cross polarization isolation better than 25 dB and a beamwidth of 0.7 degrees.

The W-band subsystem uses Millitech GOA-10 Gaussian optic antenna with polarizing grid for dual-polarization applications. The lens diameter is 1 foot (0.53 m). Specified cross polarization is better than 30 dB and the beamwidth is 0.7 degrees. Hence all three subsystems have excellent cross polarization isolation and similar beam characteristics.

Initial alignment of the antenna beams will be achieved in fabrication of the antenna system. Additional alignment will be performed during radar calibration. Figure 3 shows the profile of the antenna system for an elevation scan.

All three antennas are chosen to have the same beamwidth. Together with the beam alignment, this will ensure that the observation volume is the same for the three frequency bands.

2.2 Ku-band Radar Subsystem

The Ku-band radar subsystem employs 5.5 kW peak power, 10% duty cycle extended interaction

klystron (EIK) transmitter (Figure 4). Like the CPRS subsystems, the Ku-band radar is fully polarimetric and capable of measuring Doppler and polarimetric radar products such as depolarization ratio, (LDR within the limitations of the hybrid polarization scheme, Matrosov (2002)), differential reflectivity (ZDR), differential phase ϕ_{dp} and the co-polarized correlation coefficient, ρ_{hv} .

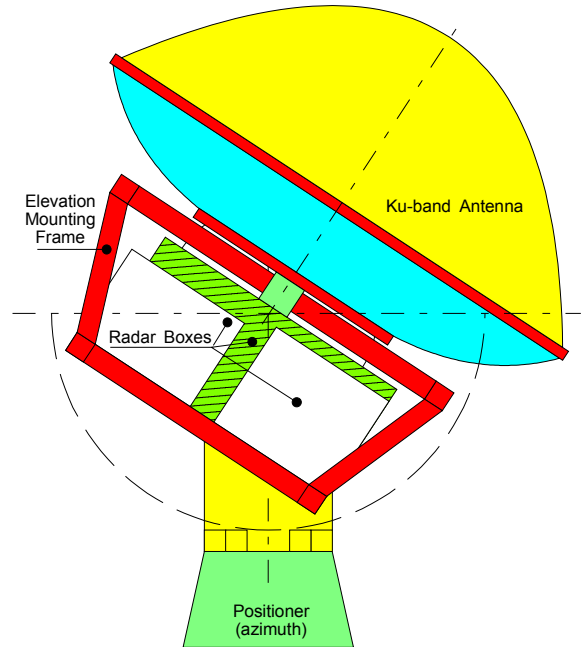


Figure 3. AMFR antenna system elevation scan.

Because the VKU-2454 extended interaction klystron (Figure 4) was originally designed for the CW applications (e.g. microwave communication links), for this radar application it was modified to operate in pulsed mode. Through this process the output peak power was increased to 5.5 kW (originally 2 kW CW) and the duty cycle was reduced to 10% (originally 100% in CW mode). This combination of long duty cycle and the peak power was used to increase sensitivity of the radar by means of pulse compression.



Figure 4. Ku-band EIK transmitter (CPI).

One problem related to aforementioned modification became evident in the operation. The VKU2454 klystron does not have a grid electrode, which is not needed for CW operation. The absence of the grid directly affects the speed of the current shutdown in the tube, and prolongs the pulse sent from the radar. Even without an input signal, the tube was generating strong noise. When enabled, the gain of the tube is 70 dB. Measurements have shown that the tube has substantial gain of 50 dB even 4 μ s after being disabled (ringing, see Figure 5, red line), for a 1 μ s long pulse (blue line in Figure 5). Due to the ringing effect there is significant power sent before and after the wanted pulse (red line). Since the ringing is not correlated to the FM chirp matched filter, it affects only the sidelobe suppression in pulse compression mode, the main lobe appears not to be affected, as illustrated in Figure 6 (red line).

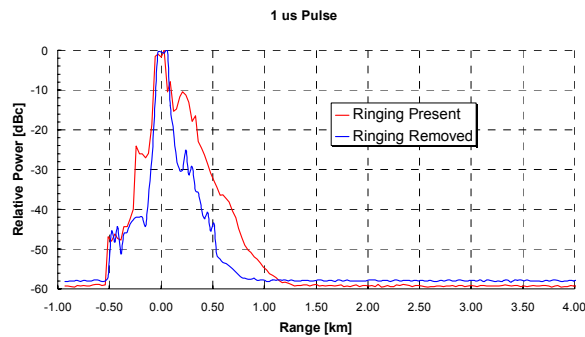


Figure 5. Single tone 1 μ s pulse sent with and without ringing removing feature.

While it is possible to remove the ringing by prolonging the receiver protector operation, this would make the radar blind for several kilometers. Rather than sacrificing close-in operation, the ringing was removed by using one extra latching circulator. This circulator is timed to direct the wanted signal towards the radar antenna and unwanted ringing into a load. The effect of this approach can be seen by comparing the red and blue lines in Figures 5 and 6. At this point it is worth mentioning that the VKU2454 is fairly inexpensive amplifier (of-the-shelf communication equipment). Even with the price of an extra latching circulator, the cost of this transmitter assembly is well below the cost of custom made radar EIK.

Figure 6 (blue line) shows the achieved pulse compression. The transmitted pulse is FM chirp 35 μ s in duration. Hamming amplitude taper is used only on the receiving side. Range sidelobe suppression is better than 45 dB. With amplitude tapering performed at the transmitter side as well, the suppression of the sidelobes reaches 65 dB.

The Ku-band subsystem of the AMFR is using three types of pulses: single tone (mostly 1 μ s or shorter), 10 μ s FM chirp and 35 μ s FM chirp. The last two are compressed to 1 μ s in order to exploit the pulse compression gain (high duty cycle transmitter).

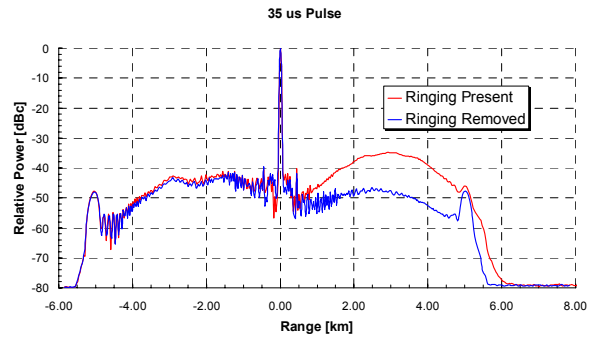


Figure 6. FM chirp (35 μ s) after pulse compression processing. Sidelobe suppression is better than 45 dB in far region (close in 40 dB). Hamming windowing was used at the receiving side only.

This is the reason why there are discontinuities in the sensitivity plot in Figure 7. First discontinuity is at 1.5 km. At this point 10 μ s FM chirp blind region ends and increased SNR can be achieved using pulse compression. Similarly, above 6 km the 35 μ s pulse blind region ends and pulse compression can take over. The complete radar image is then assembled from the sections with best SNRs.

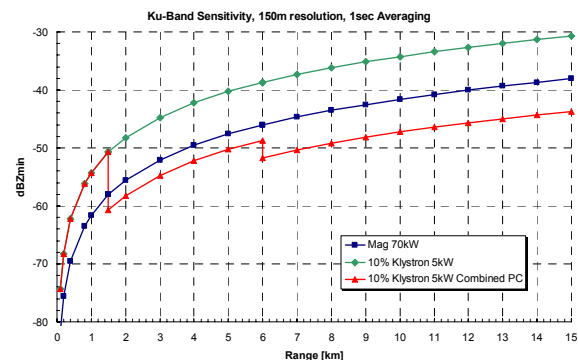


Figure 7. Calculated sensitivity for the various Ku-band transmitters (150 μ s spatial resolution, 1 s avg.).

The AMFR is for the first time employing a full internal calibration loop. Previously, the internal calibration loop was used only to monitor the changes in transmitter power output and receiver gain in between the external calibrations of the system (only power measurements). Since AMFR employs hybrid polarization, it is necessary to track the changes in phase between H and V channels of the transmitter as well. This information is then passed to the receiving processing algorithm (Matrosov (2002)). The new calibration loop is illustrated in Figure 8. The Ku-band front-end assembly is shown in Figure 9. Figure 10 shows the reflectivity plot vs. range obtained during testing at UMass in December 2004.

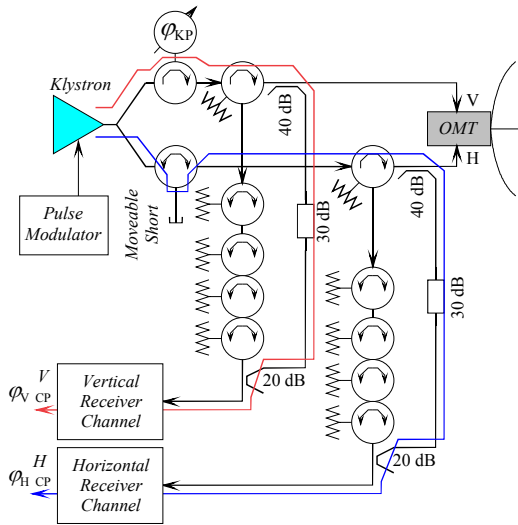


Figure 8. New Internal Calibration Loop.



Figure 9. Ku-band front-end assembly.

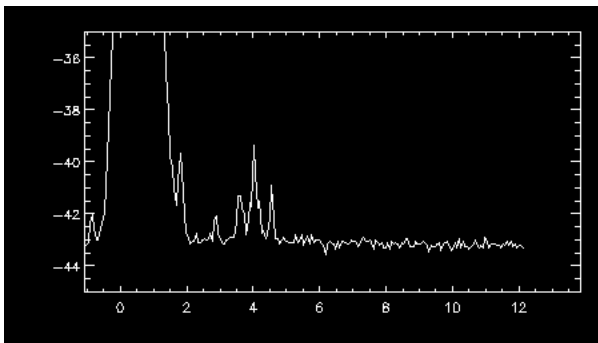


Figure 10. Reflectivity plot for zenith pointing radar antenna. The initial testing at UMass in December 2004. Horizontal axis: range in kilometers. Vertical axis: power in dB normalized to the internal calibration loop level.

2.3 Ka-band Radar Subsystem

The Ka-band subsystem of the AMFR is considerably different from its predecessor CPRS. The CPRS was employing dual magnetrons for transmitting H and V polarizations and an automatic frequency

control (AFC) loop that tunes the receiver to the magnetron frequency. Because the magnetrons are oscillators with random start-up phase, a phase correction is applied to each transmitted pulse.

The AMFR's Ka-band subsystem uses a single 1.5 kW 5% duty cycle extended interaction klystron (EIK) amplifier. The output stage is very similar to the output stage of the Ku-band subsystem. Its sensitivity is shown in Figure 11. Unfortunately, even with the pulse compression this subsystem cannot match the close in sensitivity of its predecessor CPRS. However, this design offers several advantages. Lower peak power eliminates the need for the waveguide pressurization and somewhat simplifies the antenna design. The use of the klystron also eliminates any EM interference generated by magnetron modulator (which was a major problem in CPRS).

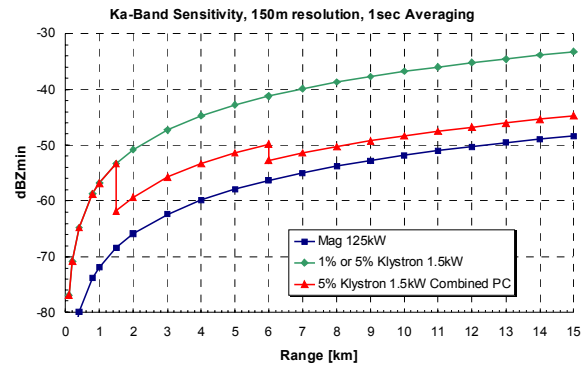


Figure 11. Calculated sensitivity for the various Ka-band transmitters (150 ms spatial resolution, 1 s avg.).

Figure 12 shows the EIK and the 5% duty cycle pulse modulator developed for its operation. The front end of the Ka-band subsystem is shown in Figure 13.



Figure 12. EIK VKQ2471 (CPI) and the pulse modulator MG1369 (Pulse Systems).

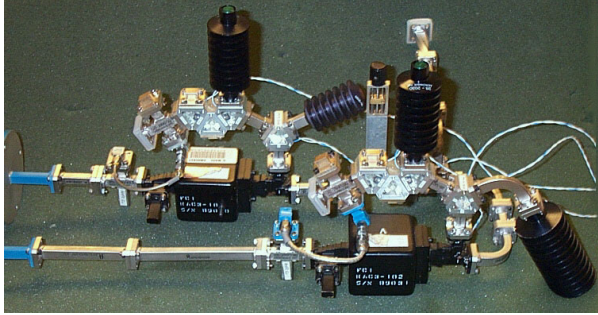


Figure 13. Ka-band front-end assembly.

2.4 W-band Radar Subsystem

Compared to CPRS, AMFR's new high duty cycle FM chirp pulse compression transmitter improves overall sensitivity at W-band by 13 dB to 20 dB, depending on the level of pulse compression achieved, resulting in the most sensitive W-band radar built to date. These enhancements significantly improve detection of weakly reflecting clouds and penetration into precipitation at low elevation angles. The key component that provides the sensitivity increase is a high duty cycle conduction-cooled klystron amplifier tube (Figure 14).



Figure 14. Conduction cooled W-band EIK VKB2461 (CPI) and the pulse modulator MG-1359 (Pulse Systems).

Figure 15 shows the sensitivity plots for the CPRS W-band subsystem and the new AMFR 5% duty cycle transmitter. It can be seen that a significant increase in sensitivity is obtained using pulse compression techniques.

Figure 16 shows the waveguide front end of the W-band subsystem. The waveguide front-end section is placed between aluminum shielding plates padded with

absorbing material. In Figure 14, V-channel front shield plate was removed for photographing purpose.

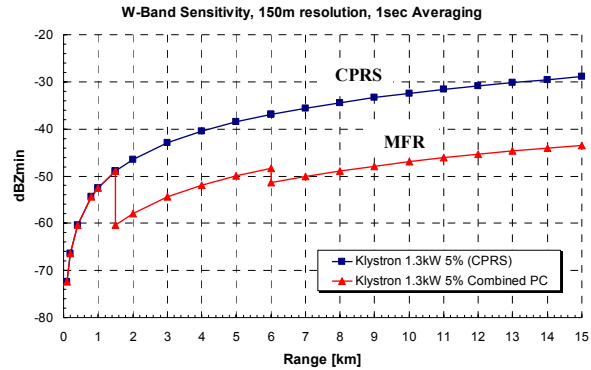


Figure 15. Calculated sensitivity for the various W-band radar systems (150 ms spatial resolution, 1 s avg.).

Similarly to Ku-band and Ka-band subsystems, the W-band subsystem also employs hybrid polarization scheme with new internal calibration loop.

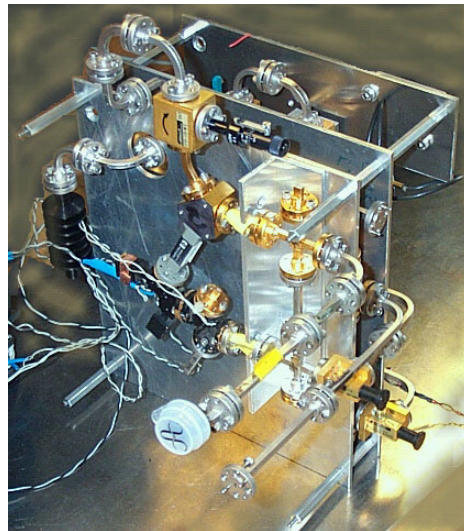


Figure 16. Front end of the AMFR's W-band subsystem. The structure has three decks: V channel (visible), H channel (middle) and LO multiplier (in the back).

2.5 Data Acquisition and Control Systems

A new Data Acquisition System (DAS) was developed for the AMFR. The immediate processing is done by three computers, individual DAS's for each subsystem (Ku, Ka and W-bands). In the DAS, three computers employ Pentek 7631 digital receiver cards for sampling and down conversion (Figure 17). The rest of the processing (e.g. pulse compression matched filters, Pulse Pair Processing) is done in software. Data rate that each of these three computers have to handle is as much as 80 Mbytes/s.

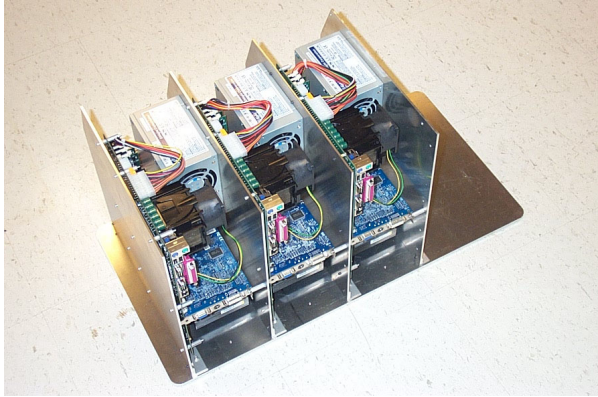


Figure 17. The Data Acquisition System Box with three PC's for immediate processing.

After initial processing, data volume is reduced such that the data rate poses no problem. Post processing products including multi-frequency velocities (DWR, differential Doppler velocities) and real time display is performed on a separate computer and poses no problem in terms of speed and data volume. The block schematic of the Data Acquisition System is shown in Figure 18.

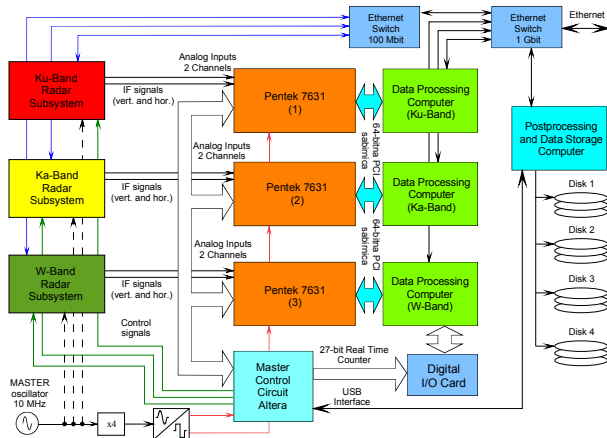


Figure 18. Block schematic of the Data Acquisition and Master Control systems.

The Master Control System is housed together with the Data Acquisition System. It consists of one PC and FPGA (Field Programmable Gate Array) circuit that generates timing signals for radar subsystems. Each radar subsystem contains an Auxiliary Control Circuit. Auxiliary control circuits accept commands and generate appropriate signals to perform requested tasks, as shown in Figure 19. The photo of the W-band Auxiliary Control Circuit is shown in Figure 20.

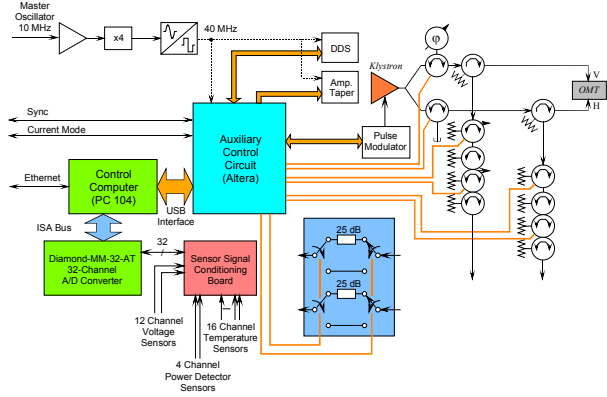


Figure 19. The block schematic of the Auxiliary Control Circuit.

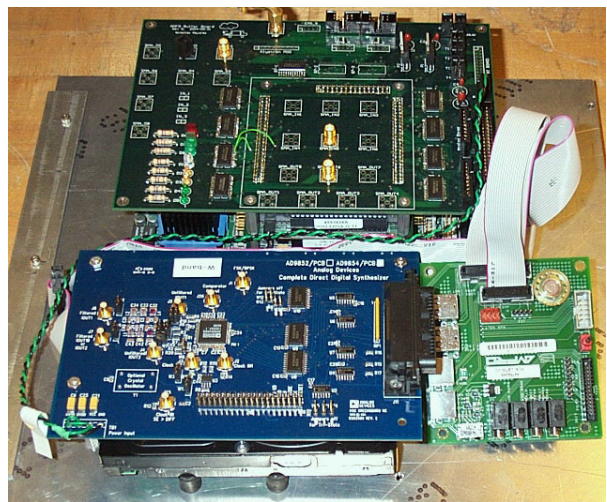


Figure 20. Auxiliary Control Circuit used in W-band subsystem.

3. CONCLUSIONS

The design and development of the Advanced Multi-Frequency Radar (AMFR) for remote sensing of clouds and precipitation has been presented in this paper. AMFR is designed as an advanced replacement for the Cloud Profiling Radar System (CPRS) built at the University of Massachusetts at Amherst. AMFR Radar System consists of three complete polarimetric subsystems, each capable of performing radial velocity measurements (Doppler). Subsystems are designed for operation in three frequency bands: Ku-band (13.4 GHz), Ka-band (35.6 GHz) and W-band (94.92 GHz). Use of a third frequency band extends dynamic range and reduces ambiguity between non-Rayleigh scattering and differential attenuation providing new measurement capabilities in mixed-phase clouds. Its modular design allows operation of a single subsystem as stand-alone single frequency radar.

AMFR system is unique in employing pulse compression in W-band with high power amplifier (1.8 kW peak power), whereas previously pulse compression was used only with low power amplifiers (under 1 W, usually solid state types). The circuits for tuning the transmitted polarization and fully complex (amplitude and phase) internal calibration loop have been employed together for the first time. Amplitude and phase of the internal calibration loop signals are used for real time tuning of the data processing algorithm. The antenna system is designed to allow collocated measurements with minimal parallax error. The antenna system operates with matched beamwidths at all three frequency bands. It is expected that this system will be fully operational and available for field deployment in the Spring of 2006.

4. REFERENCES

- [1] Andraka, R. and Berkun, A., 1999: "FPGAs Make a Radar Signal Processor on a Chip a Reality", *Proceedings of the Asilomar Conference on Signals, Systems and Computers*, Monterey.
- [2] Matrosov, S. Y., 2002: "Possibilities for Depolarization Estimates Using Simultaneous Transmission and Reception Schemes in Polarimetric Radars", in preparation.
- [3] Mooradd, D. C., 1993: "Design, Development and Construction of a Dual-frequency, Dual-polarized Millimeter Wave Cloud Profiling Radar Antenna", Master degree thesis, University of Massachusetts at Amherst.
- [4] Mudukutore, A. S., Chandrasekar, V. and Keeler, R. J., 1998: "Pulse Compression for Weather Radars", *IEEE Transactions on Geoscience and Remote Sensing*, vol. 36, No. 1, January 1998, pp. 125-142.
- [5] Sekelsky, S. M. and McIntosh, R. E., 1996: "Cloud Observations with a Polarimetric 33 GHz and 95 GHz Radar", *Meteorology and Atmospheric Physics*, vol. 58, pp. 123-140.
- [6] Sekelsky, S., Ecklund, W., Firda, J., Gage, K. and McIntosh, R., 1999: "Particle Size Estimation in Ice-phase Clouds using Radar Reflectivity Measurements Collected at 95GHz, 33GHz and 2.8GHz", *Journal of the Applied Meteorology*, 38 (8), pp. 5-28.
- [7] Sekelsky, S., Ecklund, W. and Gage, K., 2004: "Multi-frequency Radar Observations of the Melting Layer", *Proceedings of the IEEE International Geoscience and Remote Sensing Symposium*, Hamburg.
- [8] Zrnicek, D., 1996: "Simultaneous Differential Polymetric Measurements and Co-polar Correlation Coefficient Measurement", U.S. Patent no. 5.500.646, March 1996.